







Tenascin-C as a potential marker for immunohistopathology of doxorubicin-induced cardiomyopathy

Tatsuya Nishikawa ^{1,2,†}, Mikio Shiba ^{3,4,†}, Yoshihiko Ikeda⁵, Keiko Ohta-Ogo ⁵, Takumi Kondo³, Tomoka Tabata³, Toru Oka^{1,6}, Wataru Shioyama⁷, Hironori Yamamoto¹, Taku Yasui¹, Yoshiharu Higuchi⁴, Hatsue Ishibashi-Ueda^{5,8}, Keiichiro Honma⁹, Chisato Izumi¹⁰, Shuichiro Higo ^{3,11}, Kinta Hatakeyama ^{5,*}, Yasushi Sakata ³, and Masashi Fujita^{1,*}

¹Department of Onco-Cardiology, Osaka International Cancer Institute, 3-1-69, Otemae, Chuo-ku, Osaka City, Osaka 541-8567, Japan; ²Department of Cardiovascular Medicine, Akashi Medical Center, Hyogo, Japan; ³Department of Cardiovascular Medicine, Osaka University Graduate School of Medicine, Suita, Osaka, Japan; ⁴Cardiovascular Division, Osaka Police Hospital, Osaka, Japan; ⁵Department of Pathology, National Cerebral and Cardiovascular Center, 6-1, Kishibeshinmachi, Suita, Osaka 564-8565, Japan; ⁶Onco-Cardiology Unit, Department of Internal Medicine, Saitama Cancer Center, Saitama, Japan; ⁷Department of Internal Medicine, Division of Cardiovascular Medicine, Shiga University of Medical Science, Shiga, Japan; ⁸Department of Pathology, Hokusetsu General Hospital, Takatsuki, Osaka, Japan; ⁹Department of Pathology, Osaka International Cancer Institute, Osaka, Japan; ¹⁰Department of Heart Failure and Transplantation, National Cerebral and Cardiovascular Center, Suita, Osaka, Japan; and ¹¹Department of Medical Therapeutics for Heart Failure, Osaka University Graduate School of Medicine, Suita, Osaka, Japan

Received 31 October 2022; revised 9 September 2023; accepted 6 October 2023; online publish-ahead-of-print 9 October 2023

Handling Editor: Daniel FJ Ketelhuth

Aims

Doxorubicin is used in classical chemotherapy for several cancer types. Doxorubicin-induced cardiomyopathy (DOX-CM) is a critical issue among cancer patients. However, differentiating the diagnosis of DOX-CM from that of other cardiomyopathies is difficult. Therefore, in this study, we aimed to determine novel histopathological characteristics to diagnose DOX-CM.

Methods and results

Twelve consecutive patients with DOX-CM who underwent cardiac histopathological examination in two medical centres were included. Twelve patients with dilated cardiomyopathy, who were matched with DOX-CM patients in terms of age, sex, and left ventricular ejection fraction, formed the control group. Another control group comprised five consecutive patients with cancer therapy-related cardiac dysfunction induced by tyrosine kinase inhibitors or vascular endothelial growth factor inhibitors were the controls. The positive area of tenascin-C, number of infiltrating macrophages, and presence of p62- and ubiquitin-positive cardiomyocytes were evaluated. Human-induced pluripotent stem cell-derived cardiomyocytes (hiPSC-CMs) were used for *in vitro* investigation. The myocardium exhibited significantly greater tenascin-C-positive area and macrophage number in the DOX-CM group than in the control groups ($P < 0.01$). The tenascin-C-positive area correlated with the number of both CD68- and CD163-positive cells ($r = 0.748$ and $r = 0.656$, respectively). Immunostaining for p62 was positive in 10 (83%) patients with DOX-CM. Furthermore, western blotting analysis revealed significant increase in tenascin-C levels in hiPSC-CMs upon doxorubicin treatment ($P < 0.05$).

Conclusion

The combined histopathological assessment for tenascin-C, macrophages, and p62/ubiquitin may serve as a novel tool for the diagnosis of DOX-CM. Doxorubicin may directly affect the expression of tenascin-C in the myocardium.

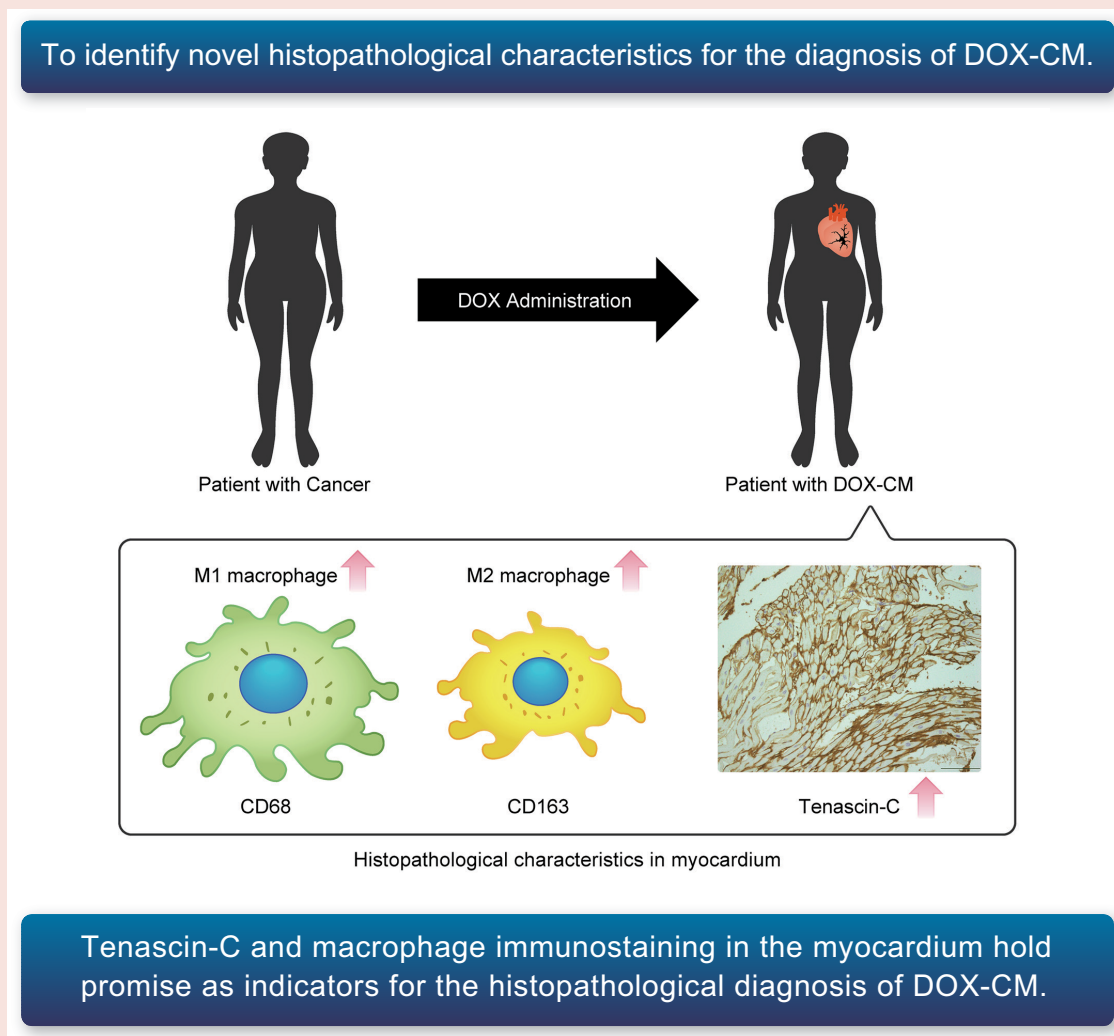
* Corresponding authors. Tel: +81 6 6945 1181, Fax: +81 6 6945 1900, Email: fujita-ma@mc.pref.osaka.jp (M.F.); Tel: +81 6 6170 1069, Fax: +81 6 6170 1956, Email: kpathol@ncvc.go.jp (K.H.)

† The first two authors contributed equally to the study.

© The Author(s) 2023. Published by Oxford University Press on behalf of the European Society of Cardiology.

This is an Open Access article distributed under the terms of the Creative Commons Attribution-NonCommercial License (<https://creativecommons.org/licenses/by-nc/4.0/>), which permits non-commercial re-use, distribution, and reproduction in any medium, provided the original work is properly cited. For commercial re-use, please contact journals.permissions@oup.com

Graphical Abstract



Histopathological characteristics of doxorubicin-induced cardiomyopathy. In the doxorubicin-induced cardiomyopathy group, the myocardium showed a higher % positive area of tenascin-C and an increased number of macrophages compared with the control group. These findings provide supportive evidence for the histopathological diagnosis of doxorubicin-induced cardiomyopathy in this study. DOX-CM, doxorubicin-induced cardiomyopathy

Keywords

Doxorubicin • Cardiotoxicity • Tenascin-C

Introduction

Doxorubicin is an effective anti-tumour agent used to treat a wide variety of cancers, including breast cancer, lymphoma, sarcoma, and gynaecological cancers.¹ However, dose-dependent progression of left ventricular (LV) myocardial damage remains the most serious adverse effect of doxorubicin-based chemotherapy, which can eventually lead to heart failure (HF) even years after completion of chemotherapy.^{2–4} The maximum cumulative lifetime dose of doxorubicin should be limited to 400–500 mg/m².^{2,5,6} In addition, doxorubicin-induced LV myocardial damage does not respond well to conventional pharmacotherapy and is associated with poor prognosis. Therefore, early detection of mild LV myocardial damage due to doxorubicin cardiotoxicity is important and may help predict future myocardial damage in the entire left

ventricle, facilitating early therapeutic intervention for LV myocardial damage.⁷ Recently, early detection of doxorubicin-induced cardiomyopathy (DOX-CM) has been demonstrated using cardiac troponin I measurement and global longitudinal strain in echocardiography.^{8–10}

An endomyocardial biopsy (EMB) is also useful to diagnose and assess myocardial damage. DOX-CM-induced vacuolation, inflammation, cardiomyocyte degeneration/necrosis/apoptosis, displacement of alignment, replacement macrophage/fibroblast infiltration, and hypertrophy have been reported in rats.¹¹ However, histopathological investigations of DOX-CM in humans are lacking. Although vacuolation and degeneration of the myocardium are typically observed, it is sometimes challenging to exclude other cardiomyopathy.^{12–14} This study aimed to identify a new marker for the diagnosis and/or prognostic assessment of DOX-CM via histopathological investigation.

Methods

Human samples

The use of patient-derived samples was approved by the Ethics Committee of Osaka International Cancer Institute Hospital (No. 20211), National Cerebral and Cardiovascular Center Hospital (No. R21084), and Osaka University Hospital (No. 15337(T3)-11). This investigation conformed to the ethical guidelines for medical and health research involving human subjects in Japan and all principles outlined by the Declaration of Helsinki.

Patients

We recruited 12 patients diagnosed with DOX-CM. Four consecutive patients with DOX-CM from the Osaka International Cancer Institute were included. Among them, samples from three patients were collected through EMB and from one patient through necropsy. We also included eight patients with DOX-CM diagnosed at the National Cerebral and Cardiovascular Center. Among the consecutive 18 clinically suspected patients with DOX-CM who underwent EMB or surgical biopsy, we excluded 2 patients with an episode of cardiac failure before doxorubicin induction, 2 patients with a suspected cause of other cardiomyopathies (myocardial infarction, hypertrophic cardiomyopathy, and chronic atrial fibrillation), and 2 patients with insufficient clinical data. Thus, a total of 12 patients underwent biopsy between 2013 and 2023 in the DOX-CM study.

Five patients with cancer who underwent EMB to assess drug-induced cardiomyopathy caused by tyrosine kinase inhibitor and vascular endothelial growth factor (VEGF) inhibitor, diagnosed at the Osaka International Cancer Institute, were selected as control patients with cancer but without doxorubicin treatment [Ctrl-cancer therapy-related cardiac dysfunction (CTRCD) group]. The specific drugs used in the control group are listed in [Supplementary material online, Table S1](#).

Additionally, we included a control group consisting of 12 patients diagnosed with dilated cardiomyopathy (DCM), who were matched with the DOX-CM group for age, sex, and LV ejection fraction (LVEF). These patients were diagnosed at the National Cerebral and Cardiovascular Centre through biopsies conducted between 2019 and 2021 (referred to as the Ctrl-DCM group). We ensured complete matching of sex for each patient, and the age difference within each pair was less than 5 years. The median difference in LVEF between each pair was 1% [interquartile range (IQR), 0–5%] (see [Supplementary material online, Table S2](#)).

Measurement

We retrospectively collected data from the time of doxorubicin introduction to index hospitalization for cardiomyopathy, baseline clinical characteristics, and echocardiography findings from medical records. Left ventricular ejection fraction was measured using the modified Simpson's method.

Immunohistochemical staining

Paraffin-embedded cardiac specimens were cut into 4 μm -thick slices and observed after haematoxylin and eosin (HE) and Masson's trichrome (MT) staining. All slides of deparaffinized cardiac specimens were incubated with primary antibodies detecting CD68 (#M0814, diluted 1:1000; Agilent Technologies Inc., Santa Clara, CA, USA), CD163 (#ab74604, diluted 1:10; Abcam, Cambridge, UK), tenascin-C (TNC) (4F10TT clone, #10337, diluted 1:1000; Immuno-Biological Laboratories, Gunma, Japan), p62 (#sc-28359, diluted 1:50; Santa Cruz Biotechnology Inc., TX, USA), and ubiquitin (#Z0458, diluted 1:500; Agilent Technologies Inc., CA, USA). Antibody binding was visualized

using the avidin–biotin complex method, according to the manufacturer's instructions (Vectastain ABC; Vector Laboratories, CA, USA). Nuclear staining was performed with Meyer's haematoxylin. A negative control from which the primary antibody was omitted was included.

Analyses of the inflammatory cell infiltrate and tenascin-C expression

CD68- and CD163-positive infiltrating cells were counted in each sample area at a magnification of 100 \times in four randomly selected fields by two pathologists (Y.I. and K.H.) in a blinded manner. Positive cells in the vessels were excluded from the total count. Finally, the number of positive cells/0.1 mm^2 was calculated. The area fraction of TNC was quantitatively measured as the percentage of the TNC-positive area using ImageJ software (National Institutes of Health, MD, USA).¹⁵

Analysis of collagen in the myocardium

To analyse myocardial fibrosis, we employed the Picrosirius Red Stain Kit (#24901-250, Polysciences, Inc., PA, USA). The staining procedure was conducted following the manufacturer's instructions. Subsequently, we captured images of the picrosirius red-stained collagen fibres using a light microscope and quantified the area exhibiting red staining. Moreover, we employed a polarized microscope to separately quantify Type I collagen (orange-red) and Type III collagen (yellow-green) areas using ImageJ software.

Generation of human-induced pluripotent stem cells and differentiation to cardiomyocytes

Human-induced pluripotent stem cells were generated from peripheral blood mononuclear cells, which were separated from whole blood using Ficoll-Paque density gradient media (GE Healthcare, IL, USA) as previously described.¹⁶ Cells were reprogrammed using Sendai virus vectors (CytoTune-iPS 2.0, Sendai Reprogramming Kit; Thermo Fisher Scientific, MA, USA). Human-induced pluripotent stem cells were cultured on laminin-coated plates (iMatrix-511, MATRIXOME, Osaka, Japan) and incubated under feeder-free conditions in the medium (StemFit AK02, AJINOMOTO, Tokyo, Japan).¹⁶ Human-induced pluripotent stem cells were differentiated into cardiomyocytes (hiPSC-CMs) using a previously reported protocol.^{17,18}

The culture medium was exchanged for a differentiation medium containing RPMI 1640 medium (Thermo Fisher Scientific), recombinant human albumin (Sigma-Aldrich, Merck, Germany), and L-ascorbic acid 2-phosphate (Sigma-Aldrich). Furthermore, hiPSCs were treated with CHIR99021 (LC Laboratories, MA, USA) (Days 0–2), followed by treatment with Wnt-C59 (Selleck Chemicals, TX, USA) and XAV-939 (Cayman Chemical, MI, USA) (Days 2–4). Human iPS cell-derived cardiomyocytes were dissociated using 0.25% Trypsin-EDTA (Gibco, Thermo Fisher Scientific, USA) and replated into a 24-well plate (IWAKI, Shizuoka, Japan) pre-coated with gelatin (Nitta Gelatin, Osaka, Japan) on Day 11. These cells were incubated with Dulbecco's Modified Eagle Medium containing 10% FBS, 2 mmol/L L-glutamine (Gibco), and 1% penicillin/streptomycin.

Human doxorubicin-induced cardiomyopathy model using human-induced pluripotent stem cell-derived cardiomyocytes

After treating the hiPSC-CMs with 0 and 0.2 μM ¹⁹ doxorubicin (HY-15142, MedChemExpress, NJ, USA) for 48 h, we assessed the levels of expressed TNC proteins using western blotting. See [Supplementary material online](#) for details regarding the qPCR method.

Table 1 Patient characteristic (doxorubicin-induced cardiomyopathy vs. control groups)

	Ctrl-CTRCD (n = 5)		Ctrl-DCM (n = 12)		DOX-CM (n = 12)		P (vs. Ctrl-CTRCD)	P (vs. Ctrl-DCM)
Age	74	[42–81]	58	[42–65]	58	[37–62]	0.316	0.547
Sex							0.102	1.000
Male	0	(0)	6	(50)	6	(50)		
Female	5	(100)	6	(50)	6	(50)		
Hypertension	3	(60)	3	(25)	1	(8)	0.053	0.590
Dyslipidaemia	2	(40)	3	(25)	1	(8)	0.191	0.590
Diabetes mellitus	0	(0)	2	(17)	2	(17)	1.000	1.000
Smoking	2	(40)	5	(42)	3	(25)	0.600	0.667
History of CAD (except for MI*)	2	(40)	1	(8)	0	(0)	0.074	1.000
CKD	1	(20)	3	(25)	10	(83)	0.028	0.012
Atrial Fibrillation	1	(20)	5	(42)	4	(33)	1.000	1.000
Echocardiography								
LVDd (mm)	47	[42–48]	62	[56–66]	58	[49–64]	0.020	0.214
LVDs (mm)	34	[33–36]	52	[49–57]	52	[44–58]	0.010	0.435
LVEF (%)	48	[43–55]	27	[23–31]	30	[22–32]	0.002	0.728
IVS (mm)	7	[7–9]	8	[7–9]	7	[5–8]	0.278	0.054
PW (mm)	7	[7–9]	8	[7–9]	8	[5–8]	0.783	0.149
E/A (n = 4, 11, 9)	1.0	[0.8–1.3]	1.8	[1.1–3.2]	2.3	[1.0–3.2]	0.189	0.939
DcT (ms) (n = 5, 12, 10)	218	[196–243]	131	[115–139]	127	[101–147]	0.004	0.552
E/e' (n = 5, 12, 9)	11.2	[7.3–20.8]	12	[11–14]	21	[13–23]	0.161	0.021
LAD (mm)	37	[28–41]	45	[38–49]	38	[36–42]	0.368	0.040
Medications								
ACEi/ARB	4	(80)	5	(42)	8	(67)	1.000	0.414
Beta-blocker	2	(40)	5	(42)	7	(58)	0.620	0.684
MRA	1	(20)	4	(33)	5	(42)	0.600	1.000

Continuous data were presented as median [interquartile range, (IQR)]. The numbers of patients for E/A, E/e', and DcT are shown in the order of Ctrl-CTRCD, Ctrl-DCM, and DOX-CM, respectively. Continuous data were analysed using the Wilcoxon rank sum test. Categorical data were analysed using a two-sided Fisher's exact test.

ACEi, angiotensin-converting enzyme inhibitor; ARB, angiotensin II receptor blocker; CAD, coronary artery disease; CKD, chronic kidney disease; DcT, deceleration time; DOX-CM, doxorubicin-induced cardiomyopathy; IVS, interventricular septum; LAD, left atrial diameter; LVDd, left ventricular end-diastolic diameter; LVDs, left ventricular end-systolic diameter; LVEF, left ventricular ejection fraction; PW, posterior wall; MI, myocardial infarction; MRA, mineral corticoid antagonist.

*There was no patient with myocardial infarction which could affect the increase in TNC.

Western blotting

Total protein was collected from hiPSC-CM lysates. The concentration of each lysate was determined using a bicinchoninic acid (BCA) Protein Assay Kit (Thermo Fisher Scientific). The lysate samples were mixed with 4x Laemmli sample buffer (Bio-Rad, CA, USA) containing mercaptoethanol (2.5%). After blocking the transferred membrane with 3% skim milk for 1 h, the membrane was incubated with the primary antibody at 4°C overnight, followed by incubation with the secondary antibody at room temperature (25°C) for 45 min. After using ECL or ECL Prime reagent (GE Healthcare, IL USA), western blotting images were captured using the ChemiDoc Touch Imaging System (Bio-Rad). The primary antibodies used in the study were as follows: anti-human TNC (4F10TT, #10337, diluted 1:100, Immuno-Biological Laboratories Co., Ltd), anti- α -actinin (EA-53) (#ab9465, diluted 1:2000, Abcam), anti-troponin T (#ab64623, diluted 1:1000, Abcam), and anti-glyceraldehyde-3-phosphate dehydrogenase (GAPDH) (#sc-47724, diluted 1:1000, Santa Cruz Biotechnology). For quantitative analysis of the density of the western blotting images, we used ImageJ software.

Statistical analysis

Unless otherwise specified, data are presented as medians and IQRs. All statistical analyses were performed using the GraphPad Prism 9

software (GraphPad Software, CA, USA) and JMP version 11.0 (SAS Inc., Tokyo, Japan). Continuous data were presented as median IQR, and differences were compared using a Wilcoxon rank sum test. The prevalence was expressed in percentages (%), and the categorical data were compared using the two-tailed Fisher's exact test. Statistical significance was set at $P < 0.05$.

Results

Patient's characteristics

In this study, we analysed three patient groups: DOX-CM, Ctrl-CTRCD, and Ctrl-DCM. We compared the characteristics of patients between DOX-CM and Ctrl-CTRCD as well as between DOX-CM and Ctrl-DCM. Table 1 shows that there were no significant differences in age, sex, cardiovascular risk factors, or medications at the initial histopathological diagnosis. The Ctrl-DCM group was selected after for matching age, sex, and LVEF, resulting in similar characteristics between the two groups. However, the DOX-CM group exhibited higher E/e' values and a shorter left atrial diameter (LAD) than the Ctrl-DCM group. In contrast, all members of the Ctrl-CTRCD group were female, and most echocardiographic markers indicated poorer cardiac function in the DOX-CM group than in the Ctrl-CTRCD group

Table 2 Individual status of patients with doxorubicin-induced cardiomyopathy

Age	Sex	Type of sampling	Cancer type	Total dose (mg/m ²)	Time from initial chemotherapy to biopsy	Type of heart failure	Troponin I/T (ng/mL)	BNP/NT-proBNP (pg/mL)	LVEF (%)	
1	60	F	EMB (RV)	Uterine cancer	480	240 days	First HF	0.215/–	–/1166	22
2	62	M	EMB (RV)	Malignant lymphoma	363	263 days	First HF	0.057/–	–/2040	35
3	56	M	EMB (RV)	ALL	330	14 years	Acute phase of chronic	–/0.079	1926/18187	22
4	35	F	Surgical biopsy (RV)	DLBCL	350	16 years	Acute phase of chronic	–/0.025	323/–	37
5	34	M	Surgical biopsy (LV)	Non-Hodgkin Lymphoma	200	23 years	Acute phase of chronic	–/0.015	315/–	17
6	31	F	EMB (RV)	Wilms tumour	300	27 years	Acute phase of chronic	–/–	944/–	31
7	60	F	Surgical biopsy (LV)	Breast cancer	200	15 months	First HF	0.139/–	–/242	15
8	77	F	Necropsy (LV)	Ovary cancer	95	70 days	First HF	0.022/–	–/10288	31
9	59	M	EMB (RV)	DLBCL	600	20 years	Acute phase of chronic	–/0.030	1048/–	32
10	43	M	EMB (RV)	ALL	NA	28 years	Acute phase of chronic	–/0.021	1122/–	24
11	45	M	Surgical biopsy (LV)	Wilms tumour	NA	42 years	Acute phase of chronic	–/–	343/–	30
12	74	F	EMB (RV)	DLBCL	350	14 years	Acute phase of chronic	–/–	2201/–	29

ALL; acute lymphoblastic leukaemia; BNP, brain natriuretic peptide; DLBCL, diffuse large B-cell lymphoma; EMB, endomyocardial biopsy; HF, heart failure; LV, left ventricle; LVEF, left ventricular ejection fraction; NA, not available; NT-proBNP, N-terminal pro-brain natriuretic peptide; RV, right ventricle.

(Table 1). Particularly, the LVEF of the DOX-CM group (30%) significantly differed from that of the Ctrl-CTRCD group (48%), although it was similar to that of the Ctrl-DCM group (27%).

The median age of the patients with DOX-CM was 58 (IQR, 37–62) years, and 50% were female. All patients had different types of cancer. Half of them underwent an index biopsy during the first HF admission, and the other half had acute worsening of chronic HF. Therefore, patients in the first HF group had a shorter duration between initial doxorubicin chemotherapy and index biopsy (70 days to 15 months) compared with the group of chronic HF. Additionally, all patients with DOX-CM received a total dose of doxorubicin below 500 mg/m² (Table 2). Furthermore, before the index biopsy, all patients had been confirmed to have intact coronary arteries by angiography. Among the 12 DOX-CM patients, 8 underwent myocardial sampling from right ventricular biopsy, 3 underwent surgical LV biopsy, and 1 underwent necropsy from the right and left ventricle (Table 2).

Histopathological characteristics of doxorubicin-induced cardiomyopathy samples

Representative images of HE and MT staining of DOX-CM are shown in Figure 1A and B. Doxorubicin-induced cardiomyopathy samples showed degeneration and/or hypertrophy of cardiomyocytes in HE staining and low percentages of fibrosis in MT staining.

As autophagy is one of the pathophysiologicals related to DOX-CM,^{20,21} we examined the presence of autophagy in all the biopsy samples as latent supportive histopathological biomarkers for DOX-CM. The myocardium samples of five patients (42%) who developed DOX-CM were positive for both p62 and ubiquitin in the vicinity of vacuoles, while none of Ctrl-CTRCD patients and only two out of 12 patients (17%) among the Ctrl-DCM patients showed positive staining for both p62 and ubiquitin. However, p62 expression was positive in 10 out of 12 patients (83%) in the DOX-CM group, while none in the Ctrl-CTRCD group and two (17%) in the Ctrl-DCM group showed

positive results (see Supplementary material online, Table S3). Microscopic images of p62 and ubiquitin are shown for one of the cases in Figure 1C and D.

Tenascin-C and macrophages were highly positive in the myocardium of patients with doxorubicin-induced cardiomyopathy

Twelve patients in the DOX-CM group were compared with five patients in the Ctrl-CTRCD group and 12 patients in the Ctrl-DCM group. Haematoxylin and eosin staining results of DOX-CM samples revealed infiltration of inflammatory cells. Therefore, we assessed the immunostaining of the lymphocytes and macrophages. In this study, the histopathological study of DOX-CM and the control group showed few CD3-positive lymphocytes. Interestingly, we found a significant increase in CD68- ($P < 0.001$) and CD163-positive ($P < 0.001$) macrophages compared with that in the control group (Figure 2).

Since DOX-CM myocardium was thought to be related to inflammatory reactions with macrophages, we assessed the immunostaining of TNC, which is also an inflammatory marker of the myocardium.^{15,23} The percentage of TNC-positive areas was significantly higher in the DOX-CM samples than in the control samples ($P < 0.001$) (Figure 3).

Additionally, TNC-positive areas were significantly correlated with the number of CD68- ($r = 0.748$, $P < 0.001$) and CD163-positive macrophages ($r = 0.656$, $P < 0.001$) in all samples (Figure 4).

As shown in Figure 5A, the DOX-CM group exhibit significantly lower LVEF than the Ctrl-CTRCD group, with no difference compared with the Ctrl-DCM group. We observed no correlation between TNC-positive areas and LVEF ($r = -0.278$, $P = 0.144$) (Figure 5B). Similarly, LVEF showed no correlation with the number of CD68- ($r = -0.122$, $P = 0.530$) and CD163-positive macrophages ($r = -0.161$, $P = 0.403$) (Figure 5C and D). Furthermore, considering that TNC is an extracellular matrix protein often associated with fibrosis, we investigated the relationship between TNC and fibrosis.

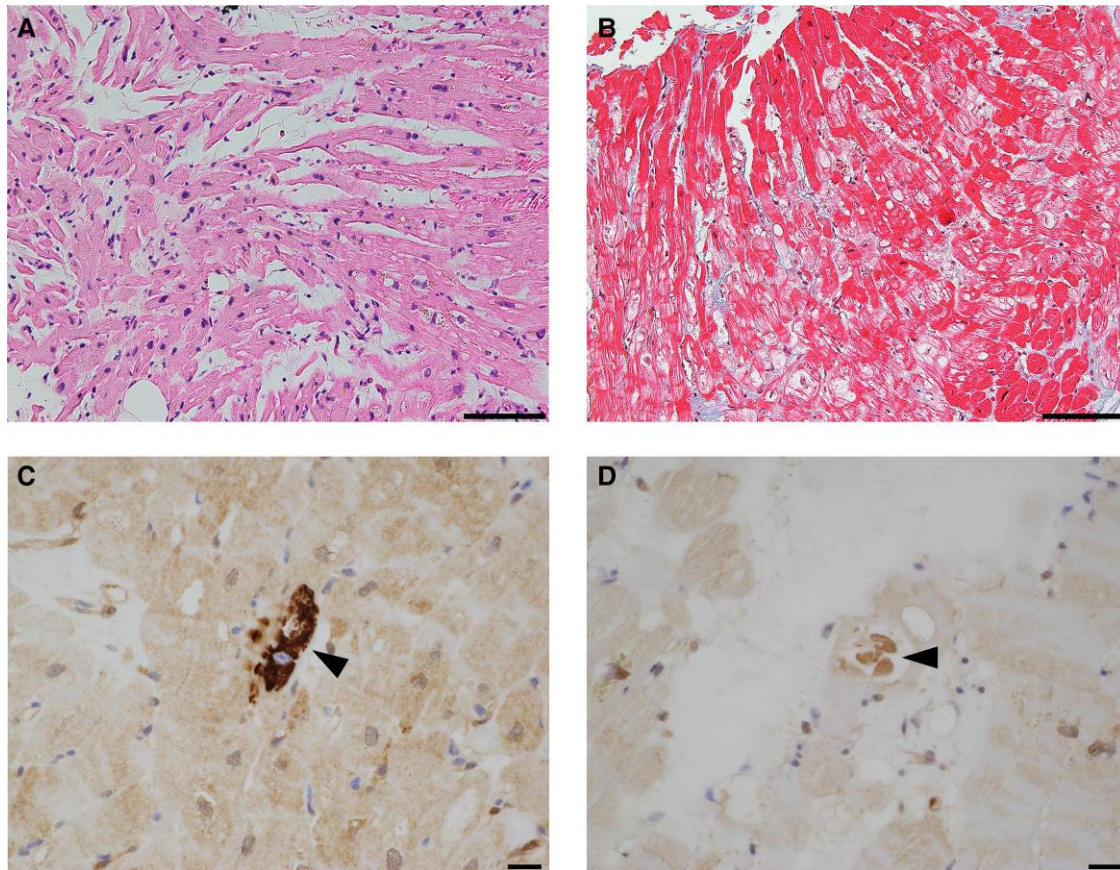


Figure 1 Representative microscopic images of doxorubicin-induced cardiomyopathy. (A) Haematoxylin and eosin staining and (B) Masson's trichrome staining with replacement fibrosis, (C) immunostaining for p62, and (D) immunostaining for ubiquitin. These show non-specific mild hyper-trophy, vacuolation, and cardiomyocyte loss with replacement fibrosis (A and B). High-power magnification shows aggregates of positive reactivity for p62 and ubiquitin in the cytoplasm with scattered distribution (C, D). The scale bar indicates 50 μm for A and B and 20 μm for C and D.

Picosirius red staining was performed to stain collagen Types I and III in the myocardium. We quantified the percentage of positive area for picosirius red staining and determined the fraction of each collagen type. However, we found no significant differences in the % positive area of picosirius red staining or the fraction of collagen Types I and III between the DOX-CM group and the control groups (see [Supplementary material online, Figure S1A and B](#)). However, neither of these measurements showed any correlation with the percentage of positive TNC area (see [Supplementary material online, Figure S1C](#)). In contrast, MT staining, a commonly used method to assess fibrosis, exhibited a significant correlation with the percentage of positive TNC area ($r = 0.479$, $P = 0.009$) (see [Supplementary material online, Figure S1D](#)). However, the percentage of positive area for MT-positive fibrosis did not correlate with the picosirius red-stained area (see [Supplementary material online, Figure S1E](#)).

Comparing the first HF and acute phase of chronic HF in DOX-CM, baseline LV end-diastolic and end-systolic diameters, the LVEF, and the number of CD68- and CD163-positive macrophages did not differ significantly (see [Supplementary material online, Figure S2](#)). Moreover, the TNC-positive area was not significantly different between those with first HF and the acute phase of chronic HF (see [Supplementary material online, Figure S3](#)).

Elucidation of tenascin-C expression in human-induced pluripotent stem cell-derived cardiomyocytes with doxorubicin administration

According to the results of the immunohistopathological assessment, it is unclear whether TNC was directly increased by doxorubicin or by the secondary products of inflammation or cell death. To confirm this, we analysed hiPSC-CMs *in vitro* using western blotting. Tenascin-C increased significantly in doxorubicin-treated cells compared with that in control cells ($P < 0.05$) ([Figure 6](#)). To gain further insights into the underlying mechanisms and relationship between TNC and inflammation, we conducted qPCR analysis of genes associated with the NF- κ B inflammatory pathway. [Supplementary material online, Figure S4](#), demonstrates that the expression of *TNF*, *TLR4*, *IL1B*, and *CCL2* was significantly upregulated upon the addition of DOX in hiPSC-CMs.

Discussion

In this study, we revealed novel histopathological characteristics of DOX-CM, such as intensive TNC with CD68- and CD163-positive

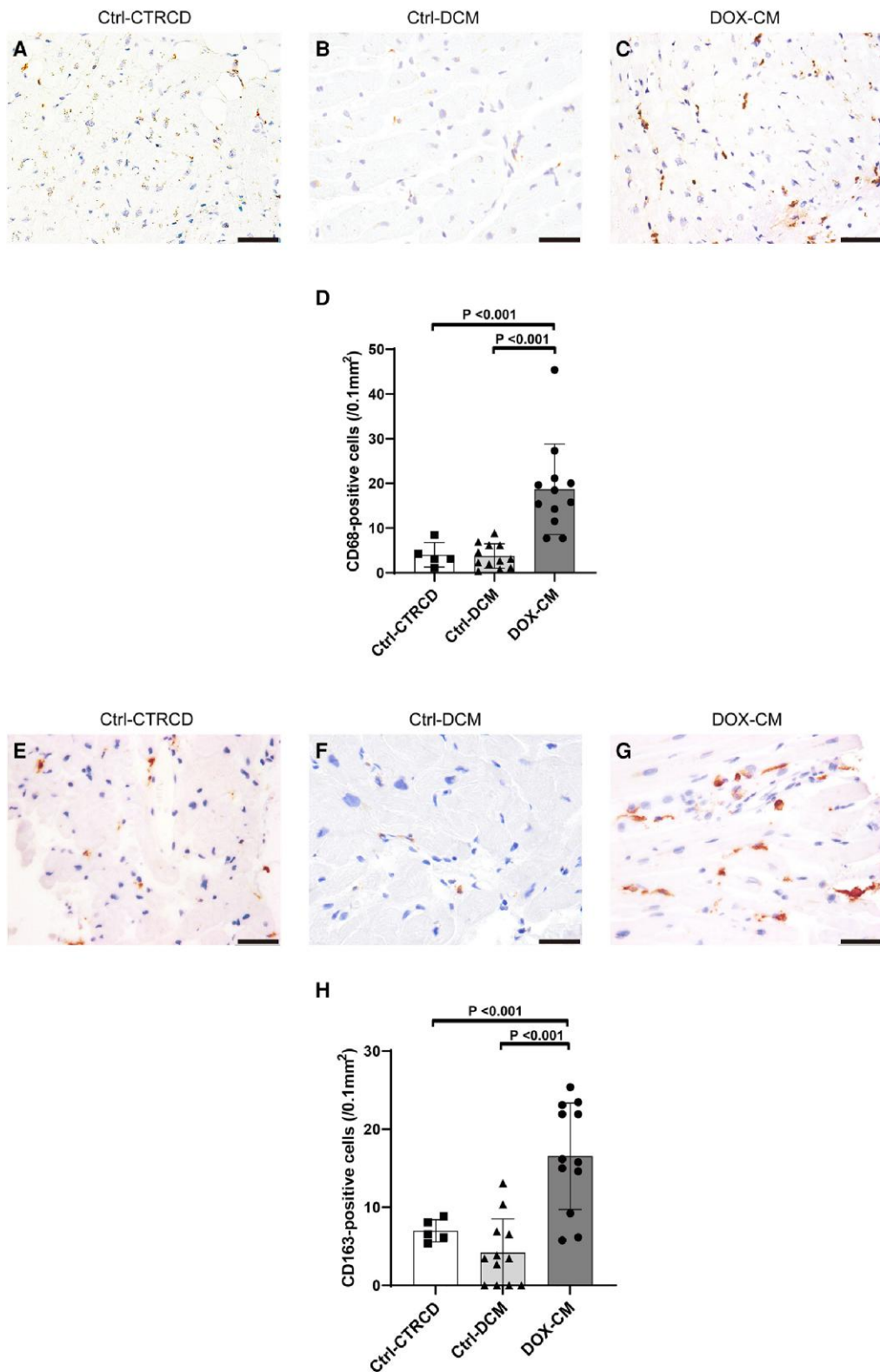


Figure 2 CD68 and CD163 expression in doxorubicin-induced cardiomyopathy and control groups. Representative photomicrographs of the myocardium obtained through a biopsy for CD68 (A, B, and C) and CD163 (E, F, and G). The number of infiltrated macrophages was significantly higher in the doxorubicin-induced cardiomyopathy group than in the control groups (D and H). *P*-values were analysed using Student's *t*-test. The scale bar indicates 50 μ m. CTRCD, cancer therapy-related cardiac dysfunction; DCM, dilated cardiomyopathy; DOX-CM, doxorubicin-induced cardiomyopathy.

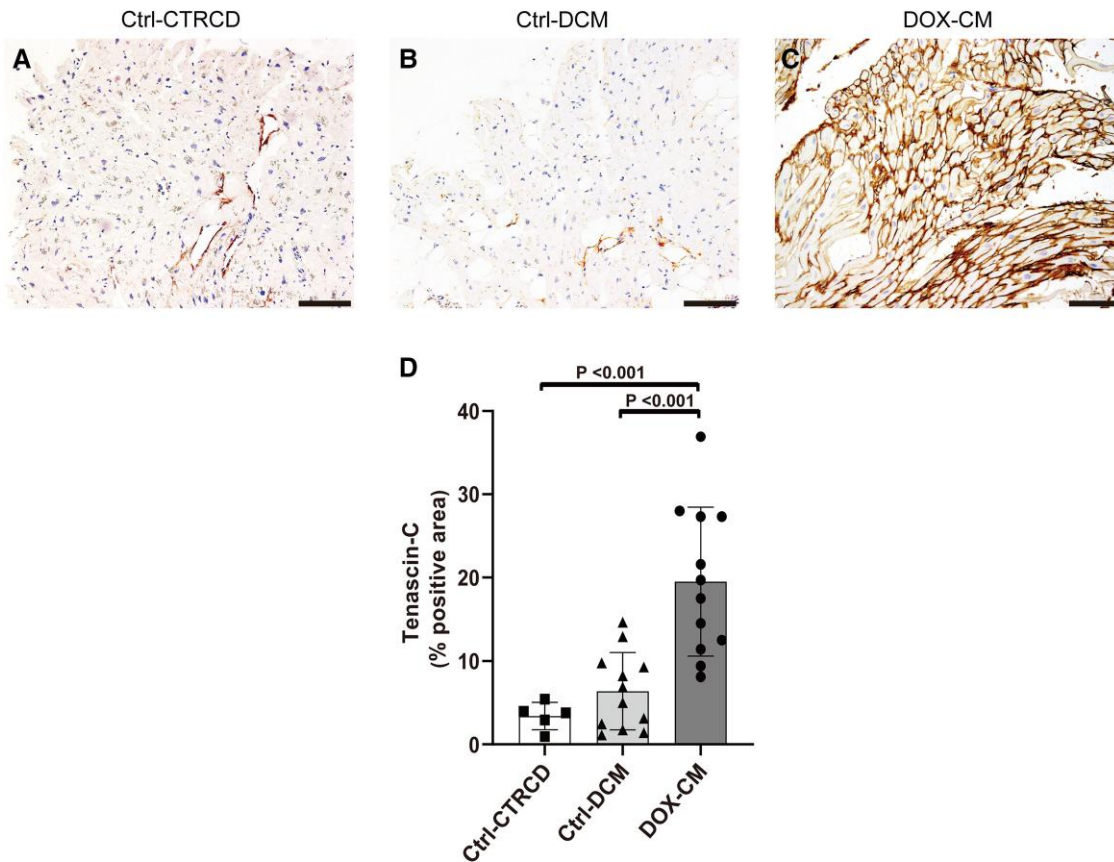


Figure 3 Tenascin-C expression in doxorubicin-induced cardiomyopathy and control groups. Representative photomicrographs of myocardium stained immunohistochemically for tenascin-C in patients in Ctrl-cancer therapy-related cardiac dysfunction (A) Ctrl-dilated cardiomyopathy (B), and doxorubicin-induced cardiomyopathy groups (C). The bar graph shows the percentage of the tenascin-C-positive area in the three groups (D). The % positive area of tenascin-C was significantly higher in the doxorubicin-induced cardiomyopathy group than in the control group. *P*-values were analysed using Student's *t*-test. The scale bar indicates 100 μ m. CTRCD, cancer therapy-related cardiac dysfunction; DCM, dilated cardiomyopathy; DOX-CM, doxorubicin-induced cardiomyopathy.

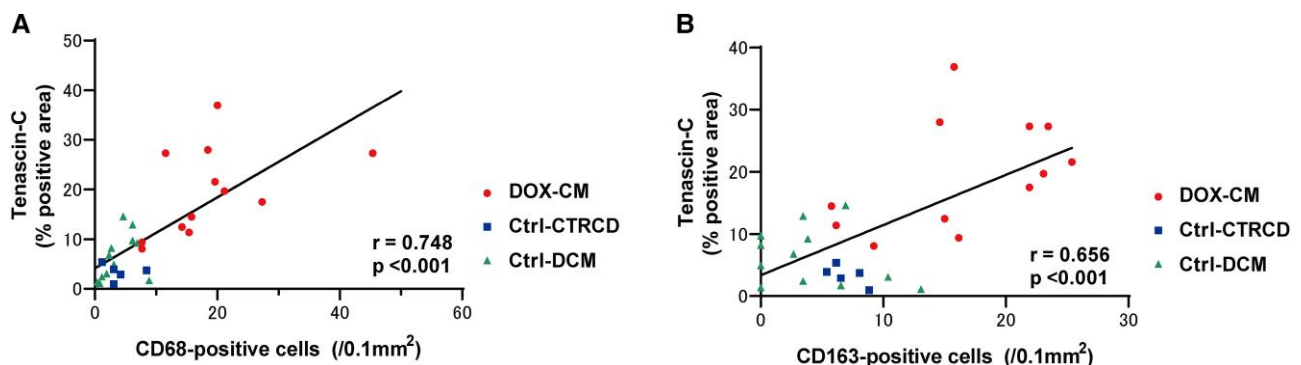


Figure 4 Correlation between CD68 expression and tenascin-C expression in all patients. The correlation between the number of infiltrated CD68-positive M1 macrophages and the percentage area of tenascin-C is shown (A, $r = 0.748$, $P < 0.001$). The correlation between the number of infiltrated CD163-positive M2 macrophages and the percentage area of tenascin-C is shown (B, $r = 0.656$, $P < 0.001$). CTRCD, cancer therapy-related cardiac dysfunction; DCM, dilated cardiomyopathy; DOX-CM, doxorubicin-induced cardiomyopathy.

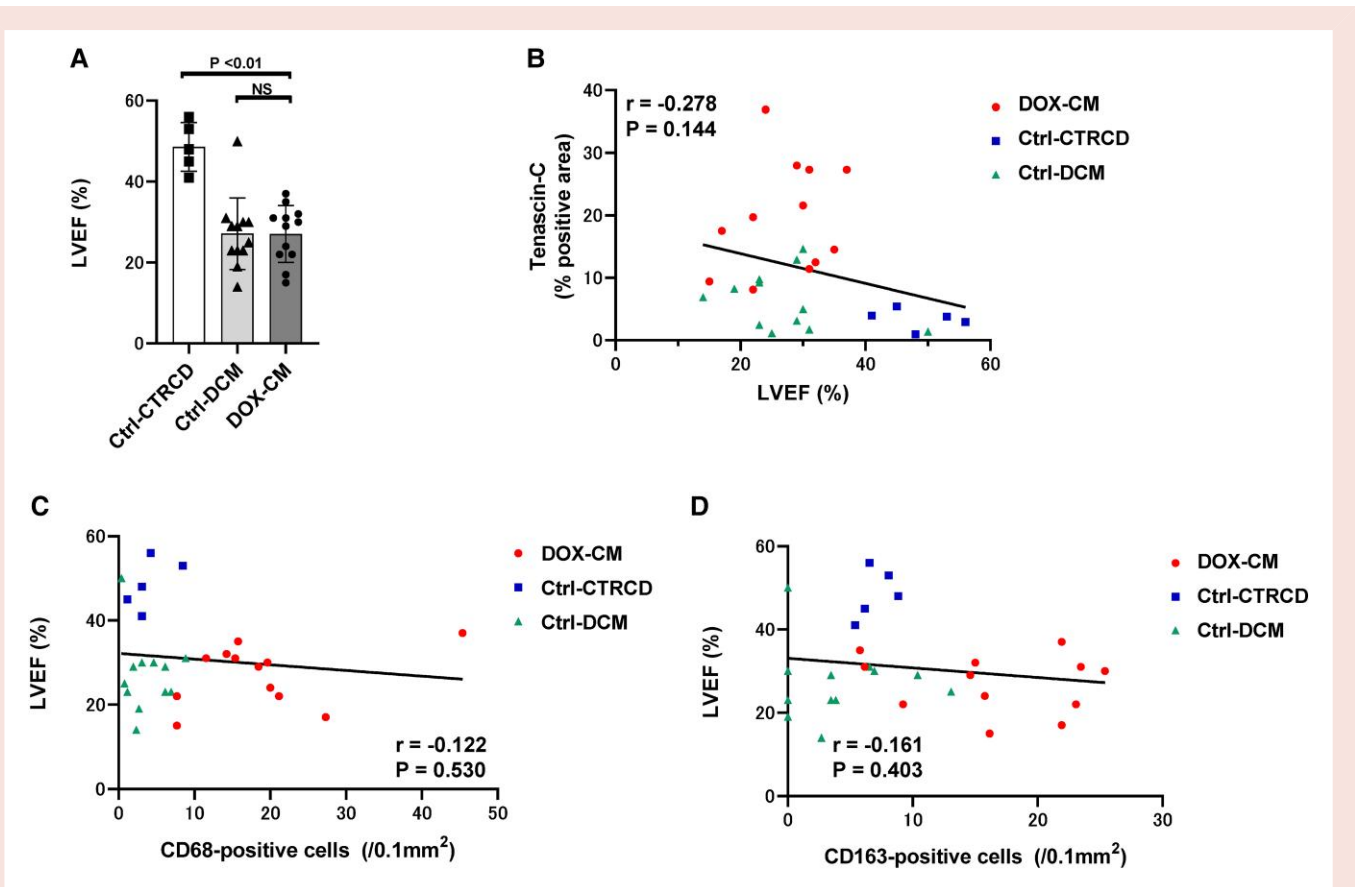


Figure 5 Relationship between the tenascin-C positive area and left ventricular ejection fraction. (A) Mean left ventricular ejection fraction of each group. The doxorubicin-induced cardiomyopathy group exhibit significantly lower left ventricular ejection fraction than the Ctrl-cancer therapy-related cardiac dysfunction group, with no difference compared with the Ctrl-dilated cardiomyopathy group. (B) In all the study patients, left ventricular ejection fraction and tenascin-C exhibited no significant relationship. (C, D) CD68- and CD163-positive macrophages were not related to left ventricular ejection fraction. CTRCD, cancer therapy-related cardiac dysfunction; DCM, dilated cardiomyopathy; DOX-CM, doxorubicin-induced cardiomyopathy; LVEF, left ventricular ejection fraction.

macrophage infiltration, followed by supportive immunohistochemistry of p62 and ubiquitin. The characteristics of DOX-CM include cardiomyocyte degeneration, hypertrophy/cytomegaly, and vacuolation¹¹; however, these were mostly non-specific to DOX-CM. Differentiation from other cardiomyopathies, such as DCM and other drug-induced cardiomyopathy, is sometimes challenging. Therefore, our findings may help in the diagnosis of DOX-CM.

Here, the main finding showed a significant increase in TNC and macrophages in the myocardium of DOX-CM. Tenascin-C, an extracellular matrix glycoprotein, is an established marker of myocardial inflammation in myocarditis, myocardial infarction, and DCM.^{15,23,24} Histopathological investigation of lymphocytic myocarditis shows CD3 (CD4 and/or CD8)-positive lymphocyte infiltration as well as CD68-positive macrophages. Therefore, the pathological mechanism of DOX-CM is completely different from that of lymphocytic myocarditis. During myocardial infarction, injured myocardial cells are eliminated by macrophages. During the repair of injured tissues with disarrangement of cardiomyocytes, fibrosis co-occurred with an increase in TNC in the border area of infarction and non-infarction.²⁵ In this study, the histopathological examination of DOX-CM showed few CD3-positive lymphocytes but increased diffuse infiltration of CD68- and CD163-positive cells. These results indicate that the

mechanisms underlying the increase in TNC in DOX-CM are similar to the biomolecular reactions that occur after myocardial infarction.

In addition, several studies have reported a relationship between TNC and macrophages. Tenascin-C induces macrophage migration to the tissue.^{26–28} Tenascin-C is thought to be related to the polarization of the M1/M2 phenotype of macrophages; however, this theory remains controversial. Sha *et al.*²⁶ reported that TNC is upregulated by ATF3, which promotes migration and reverses the M1 to M2 phenotype *via* the WNT/ β -catenin signalling pathway. By contrast, Kimura *et al.*²⁸ reported that TNC promoted macrophage transformation into an M1 phenotype *via* Toll-like receptor 4. In this study, TNC significantly correlated to both CD68- and CD163-positive macrophages, representing mostly M1 and M2 phenotypes, respectively. Therefore, in the DOX-CM myocardium, both pro-inflammatory and remodelling events occurred simultaneously. Our study is limited to support past evidence; however, we demonstrated that CD68- and/or CD163-positive macrophages with TNC could serve as supportive biomarkers for DOX-CM. Macrophages are closely related to autophagy. Polarization of M1/M2 macrophages is modified by autophagy through various mechanisms including nuclear factor- κ B (NF- κ B) degradation and the mTOR pathway.^{29,30} Shimojo *et al.*³¹ revealed a relationship between TNC and the integrin α V β 3/NF- κ B/Interleukin 6 axis in

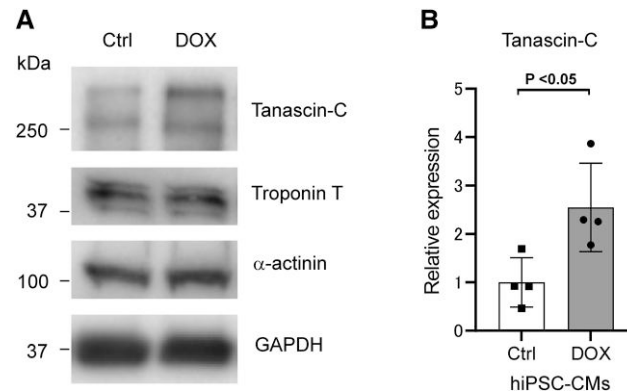


Figure 6 Western blotting in human-induced pluripotent stem cell-derived cardiomyocytes cells assessing the expression of tenascin-C by doxorubicin addition. (A) After treatment with doxorubicin, the protein levels of tenascin-C in hiPSC-CMs were assessed by western blotting using the indicated antibodies. Markers for cardiomyocytes, including troponin T and α -actinin, exhibit similar levels of expression. (B) The quantified levels of tenascin-C, normalized by GAPDH, were assessed, and tenascin-C increased after doxorubicin treatment. Troponin T and α -actinin levels showed equal differentiation of hiPSCs into cardiomyocytes. DOX, doxorubicin; hiPSC-CMs, human-induced pluripotent stem cell-derived cardiomyocytes.

cardiac fibrosis. Another study also reported the modulation of inflammatory signalling by the TNC/Toll-like receptor-4/NF- κ B axis.³² These findings suggest that TNC and NF- κ B are closely interconnected. Although direct evidence for this relationship was not established in our study, our analysis of NF- κ B signalling pathway-related gene expression deepened our understanding of the impact of DOX on TNC and NF- κ B. Therefore, considering our findings and previous reports, the intricate relationship between macrophages, TNC, and autophagy becomes apparent.

Notably, there was no considerable difference in the TNC-positive area between patients with the first HF and those in the acute phase of chronic HF. However, owing to chronic myocardial damage, the area of fibrosis was significantly higher in patients with chronic HF. Therefore, an increase in TNC may not be directly related to myocardial fibrosis. In this study, the % positive area of TNC was significantly related to fibrosis assessed by MT staining but not by picrosirius red. The underlying mechanisms for these results remain unknown within the scope of our study. Nevertheless, these findings are consistent with the notion that TNC and myocardial fibrosis may not always be directly linked.

In DOX-CM, myocardial damage is not only linked to necrosis and apoptosis but also to autophagy.^{20,21} The specific mechanisms through which autophagy affects DOX-CM are not clearly understood. Doxorubicin induces autophagy *via* dysregulation of AMP-activated protein kinase (AMPK) and mTOR; however, lysosomal dysfunction occurs owing to a decrease in the transcription factor EB, resulting in dysfunction of autophagy flux.^{20,21} During this process, p62 and ubiquitin are believed to play a role in promoting autophagy.²² Autophagy has been associated with various types of cardiomyopathies, including DCM. However, diagnostic evidence using FFPE samples has not yet been reported. Previous studies have assessed immunostaining of p62 in autophagic vacuolar cardiomyopathy, and similar findings are expected in DOX-CM in which autophagic vacuolar in the myocardium is also one of the specific histopathological characteristics.

In this study, we found positive p62 staining in cardiomyocytes in 10 out of 12 patients (83%) with DOX-CM, which was significantly higher than that observed in other control groups. Thus, immunostaining of p62 can be considered a valuable and supportive marker for the histopathological diagnosis of DOX-CM.

Although we observed a clinically important phenomenon in the DOX-CM myocardium, the molecular biological mechanisms have not yet been elucidated. Therefore, we demonstrated that doxorubicin directly induced TNC expression. In the *in vitro* assay, we found that TNC was directly induced by doxorubicin treatment in hiPSC-CMs. Nonetheless, we acknowledge that TNC increase in the myocardium might involve secondary pathways, such as interactions with other cells or inflammatory pathways. Therefore, further investigation is needed to understand the mechanisms and effects of TNC expression on DOX-CM.

The baseline characteristics (Table 1) showed that patients with DOX-CM exhibit larger LV size and lower LVEF in echocardiography at the EMB point than the control group. Therefore, we first inferred that the increased TNC was higher in the DOX-CM group owing to LV remodelling with fibrosis. However, according to the direct effects of DOX on TNC expression in our *in vitro* assays, the larger LV size and lower LVEF on echocardiography may not be the only reason for the increased percentage of the area positive to TNC in the DOX-CM group.

Since the mechanism of DOX-CM is complicated, including autophagy, necrosis, and apoptosis, further histopathological investigation in the human myocardium is needed for a more precise diagnosis of DOX-CM.

Conclusion

The present study revealed that intensive TNC immunostaining, macrophage infiltration, and a combination of autophagy-related markers, p62, and ubiquitin in the myocardium may be useful for the histopathological diagnosis of DOX-CM. The increase in TNC expression may be induced by the direct effect of doxorubicin on cardiomyocytes. Further prospective research is needed to understand the biomolecular mechanisms.

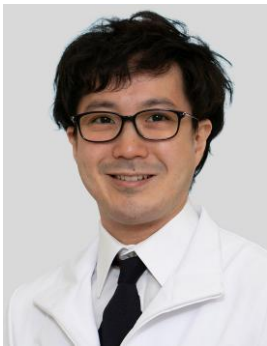
Limitations

The major limitation of the present study was the small sample size. Additionally, tissue collection through EMB can potentially lead to

sampling errors. Furthermore, because of the nature of the myocardial histopathological study, each slice of FFPE was different for each histopathological staining, which may introduce a bias in the quantitative analysis.

Here, we utilized myocardial samples from both the right and left ventricles, which can be considered a limitation. However, previous studies have reported that both ventricles are concurrently affected following DOX treatment.³³ Moreover, one sample from the DOX-CM group was obtained through necropsy, performed shortly after cardiac arrest. Notably, the values for the percentage of positive TNC area and macrophage infiltration did not exhibit outlier behaviour in our study. Considering the rarity of DOX-CM as a disease, these limitations can be deemed acceptable for the reliability of our results.

Lead author biography



Tatsuya Nishikawa, MD, PhD, is a distinguished cardiologist serving at two prestigious medical institutions in Japan: Akashi Medical Center and Osaka International Cancer Institute. With a robust background in both clinical practice and academic research, his primary focus lies HF and coronary artery disease. His current professional pursuits are dedicated to the burgeoning field of Cardio-oncology, where he passionately combines his expertise in cardiology with a keen interest in cancer-related cardiovascular issues.



Mikio Shiba, MD, PhD, FACC, serves as a cardiologist at Osaka Police Hospital, located in the vibrant city of Osaka, Japan. During his PhD course at Osaka University, he focused on research involving human induced pluripotent stem cells (hiPSCs) for patient modelling and genome editing to treat arrhythmogenic cardiomyopathy (ACM) and DCM. His professional pursuits encompass both clinical practice and a profound dedication to cutting-edge research, with a primary focus on HF

and cardiomyopathies. He is particularly driven to elucidate the intricate pathology of idiopathic DCM.

Data availability

The data sets used and analysed during the current study are available from the corresponding author upon reasonable request.

Supplementary material

Supplementary material is available at *European Heart Journal Open* online.

Author contributions

T.N., M.S., M.F., and K.H. designed the study. M.S. and T.K. T.T. performed the experiments with human iPS cells. K.H., K.H., K.O.-O., and Y.I. performed the histopathological assessments. S.H., H.I.-U., C.I., M.F., and Y.S. supervised the study. T.N., M.S., T.O., W.S., H.Y., T.Y., and Y.H. wrote the manuscript. All co-authors contributed in this research.

Funding

This work was supported by JSPS KAKENHI Grant Number 21H02915 and the Japan Agency for Medical Research and Development (21bm0804008h0005).

Conflict of interest: none declared.

References

- McGowan JV, Chung R, Maulik A, Piotrowska I, Walker JM, Yellon DM. Anthracycline chemotherapy and cardiotoxicity. *Cardiovasc Drugs Ther* 2017;**31**:63–75.
- Cardinale D, Colombo A, Bacchiani G, Tedeschi I, Meroni CA, Veglia F, Civelli M, Lamantia G, Colombo N, Curigliano G, Fiorentini C. Early detection of anthracycline cardiotoxicity and improvement of heart failure therapy. *Circulation* 2015;**131**:1981–1988.
- Pein F, Sakiroglu O, Dahan M, Lebidois J, Merlet P, Shamsaldin A, Villain E, De Vathaire F, Sidi D, Hartmann O. Cardiac abnormalities 15 years and more after adriamycin therapy in 229 childhood survivors of a solid tumor at the Institut Gustave Roussy. *Br J Cancer* 2004;**91**:37–44.
- van Dalen EC, van der Pal HJ, Kok WE, Caron HN, Kremer LC. Clinical heart failure in a cohort of children treated with anthracyclines: a long-term follow-up study. *Eur J Cancer* 2006;**42**:3191–3198.
- Lipshultz SE, Lipsitz SR, Sallan SE, Dalton VM, Mone SM, Gelber RD, Colan SD. Chronic progressive cardiac dysfunction years after doxorubicin therapy for childhood acute lymphoblastic leukemia. *J Clin Oncol* 2005;**23**:2629–2636.
- Swain SM, Whaley FS, Ewer MS. Congestive heart failure in patients treated with doxorubicin: a retrospective analysis of three trials. *Cancer* 2003;**97**:2869–2879.
- Cardinale D, Colombo A, Lamantia G, Colombo N, Civelli M, De Giacomi G, Rubino M, Veglia F, Fiorentini C, Cipolla CM. Anthracycline-induced cardiomyopathy: clinical relevance and response to pharmacologic therapy. *J Am Coll Cardiol* 2010;**55**:213–220.
- Hatazawa K, Tanaka H, Nonaka A, Takada H, Soga F, Hatani Y, Matsuzoe H, Shimoura H, Ooka J, Sano H, Mochizuki Y. Baseline global longitudinal strain as a predictor of left ventricular dysfunction and hospitalization for heart failure of patients with malignant lymphoma after anthracycline therapy. *Circ J* 2018;**82**:2566–2574.
- Saijo Y, Kusunose K, Okushi Y, al Yamada H, Toba H, Sata M. Relationship between regional left ventricular dysfunction and cancer-therapy-related cardiac dysfunction. *Heart* 2020;**106**:1752–1758.
- Tzolos E, Adamson PD, Hall PS, Macpherson IR, Oikonomidou O, MacLean M, Lewis SC, McVicar H, Newby DE, Mills NL, Lang NN. Dynamic changes in high-sensitivity cardiac troponin I levels in response to anthracycline-based chemotherapy. *Clin Oncol (R Coll Radiol)* 2020;**32**:292–297.
- Cove-Smith L, Woodhouse N, Hargreaves A, Kirk J, Smith S, Price SA, Galvin M, Betts CJ, Brocklehurst S, Backen A, Radford J. An integrated characterization of serological, pathological, and functional events in DOX-induced cardiotoxicity. *Toxicol Sci* 2014;**140**:3–15.
- Gaudin PB, Hruban RH, Beschoner WE, Kasper EK, Olson JL, Baughman KL, Hutchins GM. Myocarditis associated with doxorubicin cardiotoxicity. *Am J Clin Pathol* 1993;**100**:158–163.
- Berry GJ, Jorden M. Pathology of radiation and anthracycline cardiotoxicity. *Pediatr Blood Cancer* 2005;**44**:630–637.
- Bernaba BN, Chan JB, Lai CK, Fishbein MC. Pathology of late-onset anthracycline cardiomyopathy. *Cardiovasc Pathol* 2010;**19**:308–311.
- Shiba M, Sugano Y, Ikeda Y, Okada H, Nagai T, Ishibashi-Ueda H, Yasuda S, Ogawa H, Anzai T. Presence of increased inflammatory infiltrates accompanied by activated dendritic cells in the left atrium in rheumatic heart disease. *PLoS One* 2018;**13**:e0203756.
- Shiba M, Higo S, Kondo T, Li J, Liu L, Ikeda Y, Kohama Y, Kameda S, Tabata T, Inoue H, Nakamura S. Phenotypic recapitulation and correction of desmoglein-2-deficient cardiomyopathy using human-induced pluripotent stem cell-derived cardiomyocytes. *Hum Mol Genet* 2021;**30**:1384–1397.
- Burridge PW, Matsa E, Shukla P, Lin ZC, Churko JM, Ebert AD, Lan F, Diecke S, Huber B, Mordwinkin NM, Plews JR. Chemically defined generation of human cardiomyocytes. *Nat Methods* 2014;**11**:855–860.
- Inoue H, Nakamura S, Higo S, Shiba M, Kohama Y, Kondo T, Kameda S, Tabata T, Okuno S, Ikeda Y, Li J. Modeling reduced contractility and impaired desmosome assembly due to plakophilin-2 deficiency using isogenic iPS cell-derived cardiomyocytes. *Stem Cell Rep* 2022;**17**:337–351.
- Li J, Wang PY, Long NA, Zhuang J, Springer DA, Zou J, Lin Y, Bleck CK, Park JH, Kang JG, Hwang PM. P53 prevents doxorubicin cardiotoxicity independently of its prototypical tumour suppressor activities. *Proc Natl Acad Sci U S A* 2019;**116**:19626–19634.
- Bartlett JJ, Trivedi PC, Pulinkunil T. Autophagic dysregulation in doxorubicin cardiomyopathy. *J Mol Cell Cardiol* 2017;**104**:1–8.
- Koleini N, Kardami E. Autophagy and mitophagy in the context of doxorubicin-induced cardiotoxicity. *Oncotarget* 2017;**8**:46663–46680.
- Parry TL, Willis MS. Cardiac ubiquitin ligases: their role in cardiac metabolism, autophagy, cardioprotection, and therapeutic potential. *Biochim Biophys Acta* 2016;**1862**:2259–2269.

23. Imanaka-Yoshida K, Tawara I, Yoshida T. Tenascin-C in cardiac disease: a sophisticated controller of inflammation, repair, and fibrosis. *Am J Physiol Cell Physiol* 2020;**319**:C781–C796.
24. Imanaka-Yoshida K. Inflammation in myocardial disease: from myocarditis to dilated cardiomyopathy. *Pathol Int* 2020;**70**:1–11.
25. Imanaka-Yoshida K, Hiroe M, Nishikawa T, Ishiyama S, Shimojo T, Ohta Y, Sakakura T, Yoshida T. Tenascin-C modulates the adhesion of cardiomyocytes to extracellular matrix during tissue remodeling after myocardial infarction. *Lab Invest* 2001;**81**:1015–1024.
26. Sha H, Zhang D, Zhang Y, Wen Y, Wang Y. ATF3 promotes migration and M1/M2 polarization of macrophages by activating tenascin-C via Wnt/ β -catenin pathway. *Mol Med Rep* 2017;**16**:3641–3647.
27. Abbadì D, Laroumanie F, Bizou M, Pozzo J, Daviaud D, Delage C, Calise D, Gaits-iacovoni F, Dutaur M, Tortosa F, Renaud-Gabardos E. Local production of tenascin-C acts as a trigger for monocyte/macrophage recruitment that provokes cardiac dysfunction. *Cardiovasc Res* 2018;**114**:123–137.
28. Kimura T, Tajiri K, Sato A, Sakai S, Wang Z, Yoshida T, Uede T, Hiroe M, Aonuma K, Ieda M, Imanaka-Yoshida K. Tenascin-C accelerates adverse ventricular remodelling after myocardial infarction by modulating macrophage polarization. *Cardiovasc Res* 2019;**115**:614–624.
29. Chang CP, Su YC, Lee PH, Lei HY. Targeting NF κ B by autophagy to polarize hepatoma-associated macrophage differentiation. *Autophagy* 2013;**9**:619–621.
30. Chen W, Ma T, Shen XN, Xia XF, Xu GD, Bai XL, Liang TB. Macrophage-induced tumor angiogenesis is regulated by the TSC2-mTOR pathway. *Cancer Res* 2012;**72**:1363–1372.
31. Shimojo N, Hashizume R, Kanayama K, Hara M, Suzuki Y, Nishioka T, Hiroe M, Yoshida T, Imanaka-Yoshida K. Tenascin-C may accelerate cardiac fibrosis by activating macrophages via the integrin α V β 3/nuclear factor- κ B/interleukin-6 axis. *Hypertension* 2015;**66**:757–766.
32. Cao W, Haung H, Xia T, Liu C, Muhammad S, Sun C. Homeobox a5 promotes white adipose tissue browning through inhibition of the tenascin-C/Toll-like receptor 4/nuclear factor kappa B inflammatory signaling in mice. *Front Immunol* 2018;**9**.
33. Anghel N, Herman H, Balta C, Rosu M, Stan MS, Nita D, Ivan A, Galajda Z, Ardelean A, Dinischiotu A, Hermenean A. Acute cardiotoxicity induced by doxorubicin in right ventricle is associated with increase of oxidative stress and apoptosis in rats. *Histol Histopathol* 2018;**33**:365–378.